Formation of magnetic moments in crystalline, quasicrystalline, and liquid Al-Mn alloys

J. Hafner and M. Krajčí *
Institut für Theoretische Physik, Technische Universität Wien, Wiedner Hauptstrasse 8-10/136, A-1040 Wien, Austria
(Received 13 February 1997; revised manuscript received 8 September 1997)

We present *ab initio* investigations of the formation of magnetic moments in crystalline, quasicrystalline, and liquid Al-Mn alloys. We find that the appearance of local moments on the Mn sites is controlled by a local Stoner criterion. In the stable crystalline compound Al_6Mn strong Al-p–Mn-d hybridization enhances the formation of the structure-induced Hume-Rothery-like pseudogap at the Fermi level so that the compound is nonmagnetic. In supersaturated fcc solid solutions of the same composition this hybridization is strongly reduced; the local Mn density of states is impuritylike with a peak pinned at the Fermi level. This leads to a spin-glass-like magnetic structure with high moments on all Mn sites. Quasicrystalline and liquid alloys lie between these two extremes: In both icosahedral and decagonal quasicrystals Al-p–Mn-d hybridization is generally strong in the ideal quasicrystalline structure, but there are certain local environments that support high magnetic moments on a small number of Mn sites. The local order is reduced, but does only gradually disappear in melting. This leads to an increase of the number of magnetic sites and explains the increase of magnetic susceptiblility on melting. [S0163-1829(98)03905-8]

I. INTRODUCTION

Among the many striking physical properties of quasicrystals,[1] their magnetic behavior is perhaps the least well understood. Diamagnetism, paramagnetism, ferromagnetism, and spin-glass behavior have been reported for quasicrystalline alloys.

Ferromagnetism has been observed in Si-rich icosahedral (i) Al-Mn-Si alloys,[2,3] i-Al-Cu-Mn-Ge,[4] and decagonal (d) Al-Fe-Ce.[5] The unusual characteristics of the apparent ferromagnetism of quasicrystals are their small magnetization and comparatively high Curie temperatures. The small magnetization could be explained by the assumption that only a small fraction of the transition-metal (TM) atoms carry a large magnetic moment, while the majority of TM atoms is nonmagnetic. The existence of two classes of TM sites (magnetic and nonmagnetic) has also been confirmed by Mössbauer spectroscopy,[6] for ferromagnetic as well as for paramagnetic[7,8] quasicrystals. This has lead to speculations that the observed ferromagnetism could be associated with the presence of structural disorder in the quasicrystalline alloys[9,10] or be caused by a second crystalline ferromagnetic phase.[6,11]

Structural disorder is necessary for the formation of a spin-glass state. Spin-glass behavior in icosahedral quasicrystals has been reported for metastable Al-Mn-Ge and Al-Mn-(Si) (with low Si content) (Refs. 2,7,12,13) as well as stable Al-Pd-Mn quasicrystals.[14] Again there is evidence that only a small fraction of the Mn sites carry relatively large moments. The similarity of the magnetic properties in the icosahedral and amorphous alloys,[2,15] combined with the absence of magnetism in the structurally related crystalline compound Al_6Mn has been interpreted as further evidence for the importance of disorder for the formation of a magnetic moment in icosahedral as well as amorphous alloys.

A diamagnetic susceptibility has been measured at room temperature in the stable icosahedral Al-Cu-Fe,[16,17] Ga-Zn-Mg,[18] and Al-Pd-Mn (Refs. 19,20) quasicrystals as well as in the decagonal Al-Cu-Co and Al-Ni-Co phases.[21] With increasing temperature the diamagnetism is reduced, eventually the susceptibility even changes sign. A dramatic increase of the paramagnetic susceptibility has been observed in the melting region.[21,20]

An attempt to explain the formation of magnetic moments in quasicrystals was founded on the expectation (based on calculations for small icosahedral and octahedral Al-Mn clusters) that an icosahedral symmetry leads to a reduced p-d hybridization and hence to a high Mn density of states (DOS) at the Fermi level and the presence of a Mn moment.[22] However, this explanation is at variance with calculations for large clusters[23,24] and for periodic approximants to i-Al-Mn quasicrystals.[25] The band-structure calculations for icosahedral approximants[25–27] show that the electronic density of states at the Fermi level is reduced rather than enhanced, and this is confirmed by spectroscopic and specific-heat measurements.[1] The calculations on large clusters[23,24] show that the earlier conclusions on icosahedral site symmetry of the Mn atoms leading to formation of a magnetic moment are based on artifacts related to the small cluster size. However, Jaswal and He have also shown that moments are formed if the Mn atoms are placed on the vertices of the outer icosahedron in an icosahedral Mackay cluster.[23] This would agree with the conclusions of Moruzzi and Marcus[28] that in alloys containing transition-metal atoms there is a system-dependent critical separation of the TM atoms below which they do not carry a magnetic moment, while a moment is formed at larger separations. However, as yet, to our knowledge, no spin-polarized electronic-structure calculations for realistic quasicrystalline models that could support this conjecture have been performed.

The existence of a structure-induced Hume-Rothery-like minimum in the electronic density of states has been invoked to explain the observed diamagnetism[21,20] of quasicrystals. This argument appears to be convincing for icosahedral quasicrystals such as i-Al-Pd-Mn where both *ab initio* electronic-structure calculations[27] and soft-x-ray[29] and pho-

toelectron spectroscopy[30] confirm the existence of the Hume-Rothery pseudogap. For decagonal Al-Cu(Ni)-Co and Al-Pd-Mn on the other hand, both electronic-structure calculations[31,32] and spectroscopic measurements[33,34] agree on a high density of states at the Fermi level so that an alternative explanation for the diamagnetic susceptibility must be found. We should also mention that very recently Stadnik *et al.*[35] have attempted to reconcile the photoemission data with the existence of a structure-induced minimum in the electronic density of states (DOS). They argued that in decagonal quasicrystals a structure-induced minimum is superimposed to a smooth DOS increasing monotonously towards the Fermi energy. However, the electronic-structure calculations show that the assumption of such a background is unfounded. Anyway, the important fact is the presence of a high number of states at the Fermi energy and on that point there is agreement between theory and experiment (for a detailed comparison see Refs. 31,32).

Recent calculations of the spin-polarized electronic structure of liquid Al-Mn alloys using semiempirical tight-binding-Hubbard[36] and local-spin-density Hamiltonians[37] predicted a disordered local-moment state with large magnetic moments on *all* Mn sites. This was considered as evidence for the predominant role of topological disorder for formation of Mn moments. While these results could explain the drastic increase of the paramagnetic susceptibility on melting, the explanation of the further increase of the susceptibility in the liquid state with increasing temperature (which contradicts the Curie law) remains difficult if all Mn atoms carry a moment already just above the melting point. It would be much simpler if—as a consequence of some remanent short-range order in the liquid reminiscent of the atomic environment in the crystalline or quasicrystalline states—a distribution of magnetic and nonmagnetic sites exists in the liquid. The reduction of the short-range order with increasing temperature would then naturally lead to an increasing number of magnetic sites and thus to an increasing susceptibility.[20]

Hence there are still many open questions concerning the magnetism of quasicrystals. In the present work we have made an attempt to resolve some of the problems by performing *ab initio* self-consistent spin-polarized electronic structure calculations for crystalline solid solutions, crystalline intermetallic compounds, quasicrystalline approximants, and liquid alloys in the Al-Mn system. Our results demonstrate convincingly that in all phases, the formation of magnetic moments is governed by a local Stoner criterion $n_i(E_F)I>1$, where $n_i(E)$ is the local density of states per atom and spin and I is the Stoner intra-atomic exchange integral. This mechanism explains the nonmagnetic character of the orthorhombic compound Al_6Mn, the spin-glass behavior of a supersaturated face-centered cubic solid solution with composition $Al_{0.86}Mn_{0.14}$, the formation of large moments on a small percentage of Mn sites in some of the quasicrystalline approximants, as well as the coexistence of magnetic and nonmagnetic sites in the liquid alloys.

II. SELF-CONSISTENT REAL-SPACE TIGHT-BINDING LMTO METHOD

We have performed self-consistent *ab initio* calculations of the electronic structure and magnetic structure within the local-spin-density approximation[38] (LSDA) using a real-space tight-binding linear-muffin-tin-orbital technique (TB-LMTO).[39–41] The technique is based on a transformation of the Hamiltonian from the standard LMTO basis to the most localized tight-binding basis, resulting in a representation in terms of screened structure constant matrices and diagonal matrices determined by the LMTO potential parameters. The screened structure constants have been calculated for all topologically nonequivalent sites (within a cutoff radius equal to 2.7 times the Wigner-Seitz radius). The local spin-polarized densities of states of all inequivalent atoms are calculated using the recursion method.[42] We used typically between 20 and 80 recursion levels and the Lucchini-Nex terminator.[43] The valence charge and spin densities are constructed from moments of the local DOS, the core charge densities are obtained from scalar-relativistic calculations for the free atoms. The calculations are iterated until full self-consistency for charge and spin densities at all atomic sites has been achieved.

Our calculations have been performed in real space, i.e., only for the Γ point of the Brillouin zone of the crystal, or approximant, or of the supercell representing the substitionally disordered or liquid alloys. The elementary cells of the quasicrystalline approximants contain between 128 and 544 atoms, supercells of similar size have been used for the disordered alloys. In order to achieve a good resolution for the DOS and to reduce the effects of the periodic boundary conditions, the cell was duplicated in each direction. This multiplication of the cell does not increase the number of topologically inequivalent sites and the computer time scales linearly with the total number of atoms. The energy resolution depends on the number of recursion levels which is, however, limited by the dimensions of the model. At the end of the self-consistency cycle, the number of the recursion levels was increased to improve the resolution.

As in a disordered system it is conceivable that there are competing magnetic states with comparable total energies, the initialization of the spin-polarized calculations is important. In our calculations we have chosen to initialize the local moments at small values ($\mu<0.5\mu_B$) so that the calculation will converge to a magnetic solution only if the paramagnetic state is unstable with respect to the formation of a local moment. In this way we do not, however, explore the possible existence of metamagnetic solutions separated by a large barrier form the paramagnetic state. For all further details we refer to our previous publications.[27,31,32]

III. CRYSTALLINE AL-MN PHASES

A. Orthorhombic Al_6Mn

The electronic structure of the orthorhombic compound Al_6Mn (space-group symmetry $Cmcm$ (No. 63), 14 atoms/cell) (Ref. 44) has been discussed repeatedly in the literature.[31,45] The local atomic structure is thought to be closely related to that of the icosahedral Al-Mn and Al-Pd-Mn phases, but cannot be considered as a periodic approximant of the quasicrystalline structure. The electronic structure is characterized by a very deep pseudogap at the Fermi energy (see, e.g., Fig. 1 in Ref. 31), resulting from the coincidence of a Hume-Rothery-like structure-induced pseudogap in the Al-s,p band with the hybridization

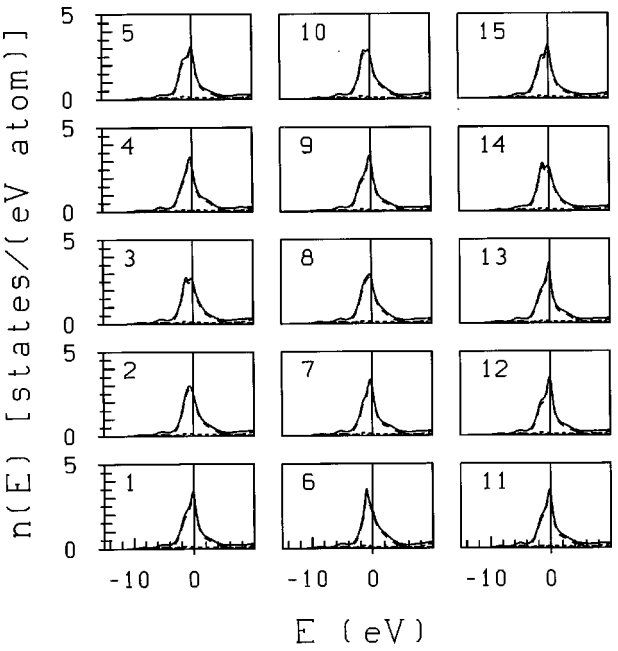

FIG. 1. Paramagnetic local electronic density of states on the Mn sites in 108-atom supercell representing an fcc $Al_{0.86}Mn_{0.14}$ solid solution.

pseudogap in the Mn-d band. The p-d hybridization also leads to an enhancement of the effective Al-pseudopotential matrix element promoting the formation of the Hume-Rothery pseudogap. The low paramagnetic DOS at the Fermi energy excludes the formation of magnetic moment on the Mn sites.

B. Face-centered-cubic $Al_{0.86}Mn_{0.14}$ solid solution

To study the effect of the local topology, we performed calculations for substitutionally disordered face-centered cubic Al-Mn with a composition close to that of the crystalline and quasicrystalline phases (i.e., at a high degree of supersaturation). Calculations for isolated impurities in an Al matrix predict magnetic moments of $\mu_{Mn}\sim 2.5$ to μ_B on the Mn sites.[46–48] Very recent calculations by Hoshino, Zeller, and Dederichs[48] have also considered the case of single Mn-Mn dimers in an Al matrix, using a Kohn-Korringa-Rostocker Green's-function method for impurities. In the impurity dimers the Mn moment is enhanced to $\mu=2.8\mu_B$ (for the nearest-neighbor dimer) and $\mu=2.7\mu_B$ (for the second-neighbor dimer). In both cases the energy is almost the same for ferro- and antiferromagnetic orientations of the moments.[48,49] Our calculations have been performed for 108-atom supercells with 15 Mn atoms distributed randomly over the sites of an fcc lattice. The paramagnetic local DOS's $n_i(E)$ show that even at this relatively high Mn concentration the Al-s,p −Mn-d hybridization remains very weak and the Mn-DOS is essentially impuritylike (i.e., it has a narrow, allmost Gaussian-like shape), with a peak at the Fermi level as expected for a half-filled d band (see Fig. 1). We also note that the Mn-d −DOS sharply peaked at the Fermi level conforms rather well with the predictions of the virtual-bound-state model.[45] Only at a very small number of sites is the peak slightly shifted from the Fermi level due to the local interactions. Hence a local Stoner criterion

TABLE I. Magnetic moments (in μ_B) on the Mn sites in a 108-atom supercell representing a face-centered-cubic Al-Mn solid solution. The numbering of the sites is the same as in the graphs showing the electronic DOS.

Site No.	Local moment	Site No.	Local moment
1	2.465	9	2.434
2	−1.984	10	−2.163
3	2.010	11	2.342
4	2.134	12	2.605
5	−2.532	13	2.406
6	1.166	14	2.099
7	2.303	15	2.436

$n_i(E_F)I(E_F)\geq 1$ with $I\sim 1$ eV/μ_B is satisfied on all Mn sites, except for atom No. 6 [Fig. 1(a)] where the DOS just fails to reach the limiting value. A spin-polarized calculation converges towards a distribution of large Mn moments with $2\mu_B\leq|\mu_i|\leq 2.6\mu_B$ on all sites satisfying the local Stoner criterion (see Table I). On the site where the condition is not satisfied, a moment develops only slowly through the covalent coupling of the d states to the spin-polarized states on the neighboring Mn atoms. Convergence is also distinctly slower on those sites where the local Stoner criterion is only marginally fulfilled. The spin-polarized DOS's (Fig. 2) show a pronounced non-rigid-band behavior: the majority-spin DOS shows always a narrower distribution (with maxima between −2.5 and −1.5 eV) than the minority-spin DOS (with peaks at about 1 eV). The local exchange splitting (measured in terms of the positions of the dominant peaks in the spin-up and spin-down DOS's) varies between $\Delta E\sim 1$ eV and $\Delta E\sim 3$ eV.

The orientation of the local moments depends on the local Mn-Mn coordinations: nearest-neighbor moments tend to

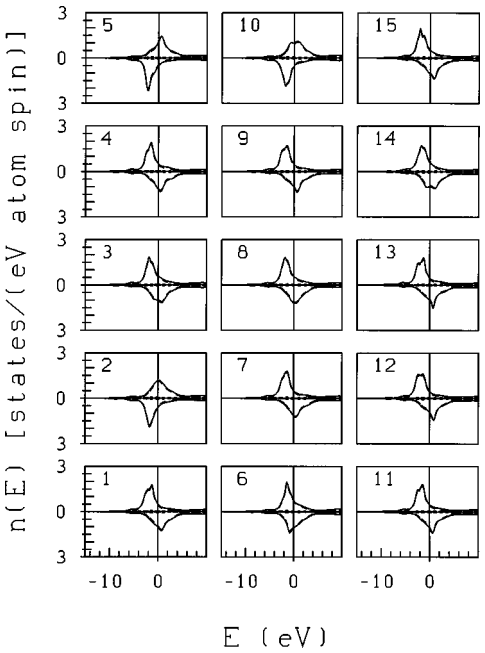

FIG. 2. Spin-polarized local electronic densities of states on Mn sites in 108-atom supercell representing an fcc $Al_{0.86}Mn_{0.14}$ solid solution. Cf. Fig. 2 for the paramagnetic DOS's.

align antiferromagnetically, next-nearest neighbors ferromagnetically. This suggests that the distance dependence of the magnetic exchange interactions is conformal with the predictions of the Ruderman-Kittel-Kasuya-Yoshida (RKKY) model.[51] Given the fact that we consider an alloy with 16 at. % Mn and in view of the very small energy differences between different spin configurations, this result is not in direct contradiction to the result of Hoshino *et al.*[48] for the isolated Mn-Mn dimers (in our recursion TB-LMTO approach we can, of course, only calculate differences in the band energies, but in the spirit of the force theorem, this can be expected to be the dominant contribution). The actual spin configuration depends to some extent on the initialization of the local moment, different initializations can lead to different energetically almost degenerate configurations. The results are entirely analogous to the recent LSDA calculations[50] for the classical spin-glass alloy Cu 5(10) at. % Mn where again an impuritylike paramagnetic Mn-DOS leads to a spin-glass state. For Cu-Mn it was also shown that if the condition of collinear orientation of magnetic moments is relaxed, the directions of the moments are also randomly distributed.[50] We would expect a similar result for the fcc Al-Mn alloy.

IV. QUASICRYSTALLINE APPROXIMANTS

A variety of quasicrystalline and approximant phases have been discovered in the binary Al-Mn and ternary Al-Pd-Mn systems. The metastable binary icosahedral phase with a composition close to Al_6Mn belongs to the simple icosahedral structures, the crystalline α-AlMn phase is a (1/1) approximant to the quasiperiodic structure. The stable ternary icosahedral phase with approximate composition $Al_{70}Pd_{22}Mn_8$ has a metastable (2/1) approximant,[52] both may be modeled in terms of projections from a six-dimensional face-centered hypercubic lattice.[53,27] The ternary decagonal phases are richer in Mn, they have a close strucural relationship with the crystalline ''Al_3Mn'' T phase,[54] the $Al_{60}Ni_4Mn_{11}$ R phase,[55] and a τ^2-inflated [τ is the Golden mean $\tau=(1+\sqrt{5})/2$] version of the R phase.[56] In the following we discuss the formation of magnetic moments on the basis of *ab initio* electronic-structure calculations for approximants.

A. Icosahedral phases

The electronic structure of a (1/1) approximant to i-AlMn has been calculated by Fujiwara.[25] The DOS is characterized by a Hume-Rothery-like pseudogap at the Fermi level, quite as in the crystalline Al_6Mn phase. This excludes the formation of a magnetic moment.

For i-Al-PdMn the electronic structure of a hierarchy of higher-order approximants has been calculated by Krajčí *et al.*[27] The calculations are based on projections from six-dimensional space with triacontahedral acceptance domains proposed by Cockayne *et al.*[53] such as to agree with the measured diffraction data. For the present purpose the most remarkable features are the low symmetry of the Mn sites and the complete absence of direct Mn-Mn neighbors (Mn atoms are surrounded on average by 7–9 Al atoms and about one Pd atom, in good agreement with extended x-ray-absorption fine-structure experiments, for further details see Krajčí *et al.*[27]). In the 2/1 to 8/5 approximants a Hume-Rothery-like pseudogap is predicted. The DOS minimum becomes deeper as the quasiperiodic limit is approached—again this suppresses the formation of the magnetic moments. However, for the 1/1 approximant (128 atoms per cell) it turns out to be difficult to meet simultaneously the requirements of the correct stoichiometry and correct topology. A model based on the same acceptance domains in six-dimensional space as the quasicrystal leads to realistic interatomic distances, but to an increased (15.6 at. % against 8.6 at. %) Mn concentration. In the electronic structure this results in an increased Mn-DOS at the Fermi level. The local DOS's at the topologically inequivalent sites are shown in Fig. 3. The Al sites are characterized by a pronounced structure-induced minimum at E_F, the maxima of the Mn-DOS's are situated 0.8–0.5 eV below E_F, only at site 1 does the value of the DOS come close to fulfilling the Stoner criterion. A spin-polarized cal-

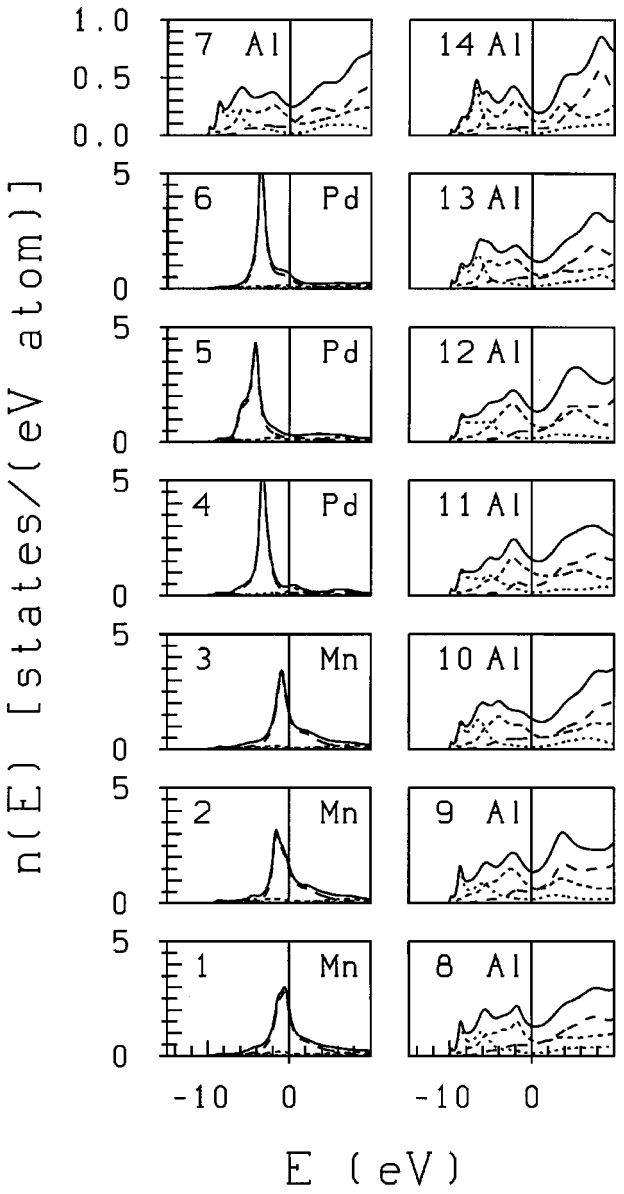

FIG. 3. Paramagnetic local densities of states on the topologically inequivalent sites of the 1/1 approximant to i-Al-Pd-Mn, as discussed in the text.

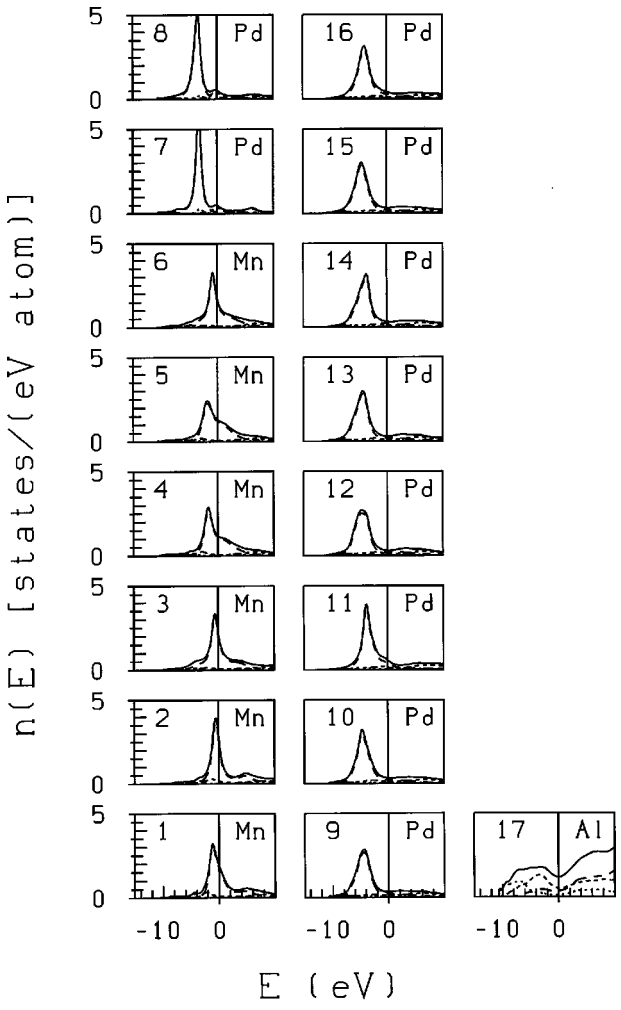

FIG. 4. Paramagnetic local densities of states on the topologically inequivalent Mn and Pd sites of the 2/1 approximant to *i*-Al-Pd-Mn. For Al only the average DOS is shown.

culation shows that as expected all sites except site 1 are nonmagnetic. Site Mn_1 is marginally magnetic, after an initialization to $0.5\mu_B$ the calculation converges to $\mu_1(\mathrm{Mn}) \sim 0.12 \pm 0.02\mu_B$.

The paramagnetic DOS calculated for the 2/1 approximant of *i*-Al-Pd-Mn (544 atoms per cell) shows a similar picture (Fig. 4). The Mn sites in the 2/1 approximant discussed here are surrounded by 7–12 Al atoms and 0–3 Pd atoms, there are no direct Mn-Mn neighbors (as in the crystalline Al_6Mn phase). A narrow local DOS peaked close to E_F is found at the Mn sites (2, 3, 6) with a small number of Al neighbors (and hence a weak Al-s,p−Mn-d hybridization) and/or 2 or 3 Pd neighbors. As in many transition metals one observes a certain repulsion of the d bands with a tendency to push the Mn band towards the Fermi level. Quite large local variations in the DOS arise from fluctuations in the local atomic environment. The Stoner criterion is satisfied for sites 2 and 3 occupied by Mn atoms. A spin-polarized calculation shows again that the sites are marginally magnetic with small moments of the order of $0.1\mu_B$.

B. Decagonal phases

Calculation of the paramagnetic electronic structure of d-Al-Pd-Mn and of related R, T, τ^2-R, and τ^2-T approxi-

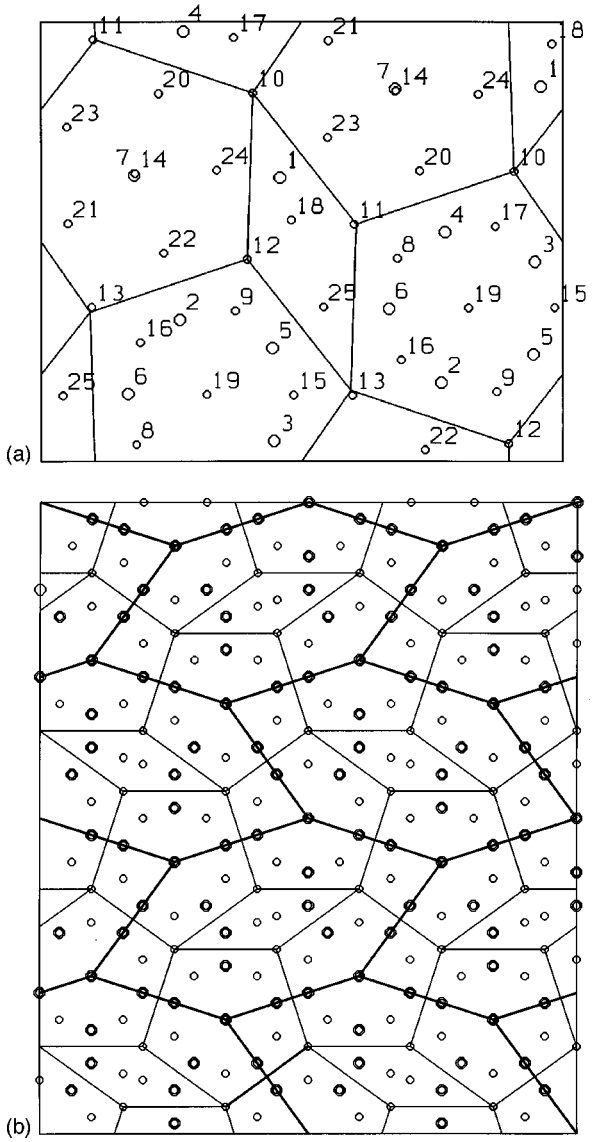

FIG. 5. Atomic structure of the T phase: (a) Projection of the positions of the atoms in half of the period on a plane perpendicular to the c axis ($\sim$ periodic axis in the quasiperiodic limit). Upper and lower half of the cell are related through a twofold screw symmetry operation. Sites 1–7 (large circles) are occupied by Mn atoms, sites 8–24 (small circles) by Al atoms. (b) Projection of a full period of four unit cells. The thick lines show the H tiles, the thin lines the decomposition of the H tiles into small pentagonal columnar clusters and thin rhombi.

mants have been performed on the basis of the decagon-pentagon-hexagon (DPH) tiling models with atomic decorations based on the pentagonal columnar clusters as proposed by Hiraga and Sun[57] and Beeli and Horiuchi,[56] slightly modified such as to lower the electronic total energy.[31] As for the icosahedral phases and for all decagonal and approximant phases, the Al-s,p band is characterized by a deep structure-induced pseudogap at the Fermi level. However, unlike in the icosahedral alloys, the Mn-d band overlaps with the Fermi level and leads to a relatively high total DOS. The investigation of the local DOS shows that with the chemical decoration optimized such as to lower the band energy (and hence the DOS at the Fermi level), all atomic sites fail to satisfy the local Stoner criterion (see Ref. 31, Fig. 9). How-

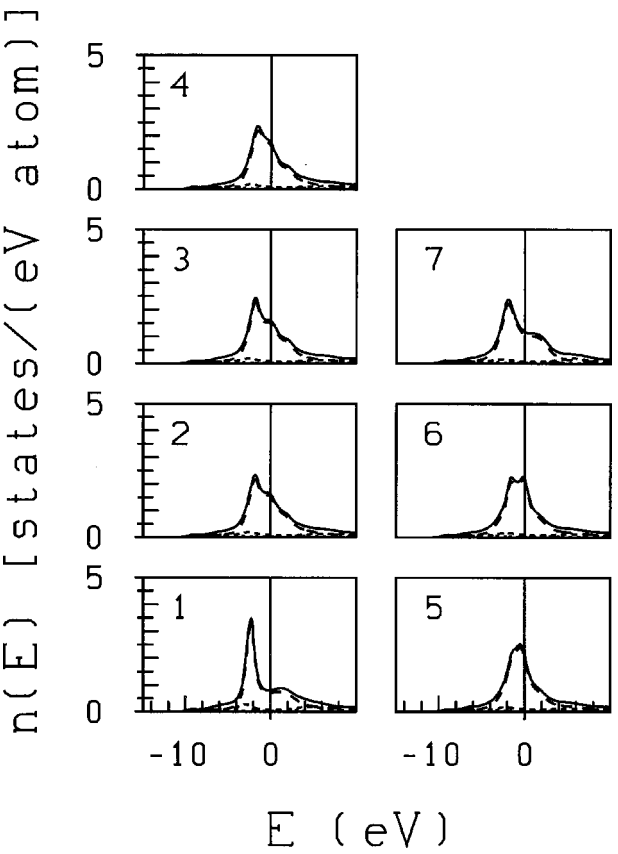

FIG. 6. Paramagnetic local electronic densities of states on the Mn sites of *T*-phase Al-Mn.

ever, it is concievable that a slight change in the atomic decoration leads to the formation of local moments on certain Mn sites. This possibility is explored in detail for the *R* and *T* phases.

The model for the structure of the *T* phase is based on structural data from the single-crystal x-ray refinement of Hiraga *et al.*[58] The orthorhombic unit cell with lattice parameters $a=12.59$ Å, $b=14.8$ Å, $c=12.42$ Å contains 156 atoms, the space group is *Pnma* (No. 62). The structural refinement leads to a mixed, respectively, fractional site occupation. These occupations have been replaced by integer values such that the columnar pentagonal clusters constituing the backbone of the DPH-tiling decoration have full pentagonal symmetry. Figure 5 shows a projection of the *T*-phase structure and its decomposition into *H* tiles and small pentagonal columnar clusters, the composition is $Al_{79.5}Mn_{20.5}$.

Figure 6 shows the paramagnetic local DOS on the seven crystallographically inequivalent Mn sites. On sites 1 to 4 and 7 the Mn-*d* DOS is quite asymmetric, with a peak about 1 eV below the Fermi level. On sites 5 and 6 on the other hand, the DOS is more symmetric and the local Stoner criterion is marginally satisfied. A spin-polarized calculation converges very slowly to substantial moments at sites 5 and 6 ($\mu_5=0.66\mu_B$, $\mu_6=1.00\mu_B$) and a small moment at site 2, all other moments are smaller than $0.1\mu_B$ (positive or negative), in the corresponding spin-polarized local DOS (not shown) there is again some evidence for a non-rigid-band behavior.

The *R* phase of Al-Mn has orthorhombic symmetry, space group *Cmcm* (No. 63). The unit cell with lattice parameters

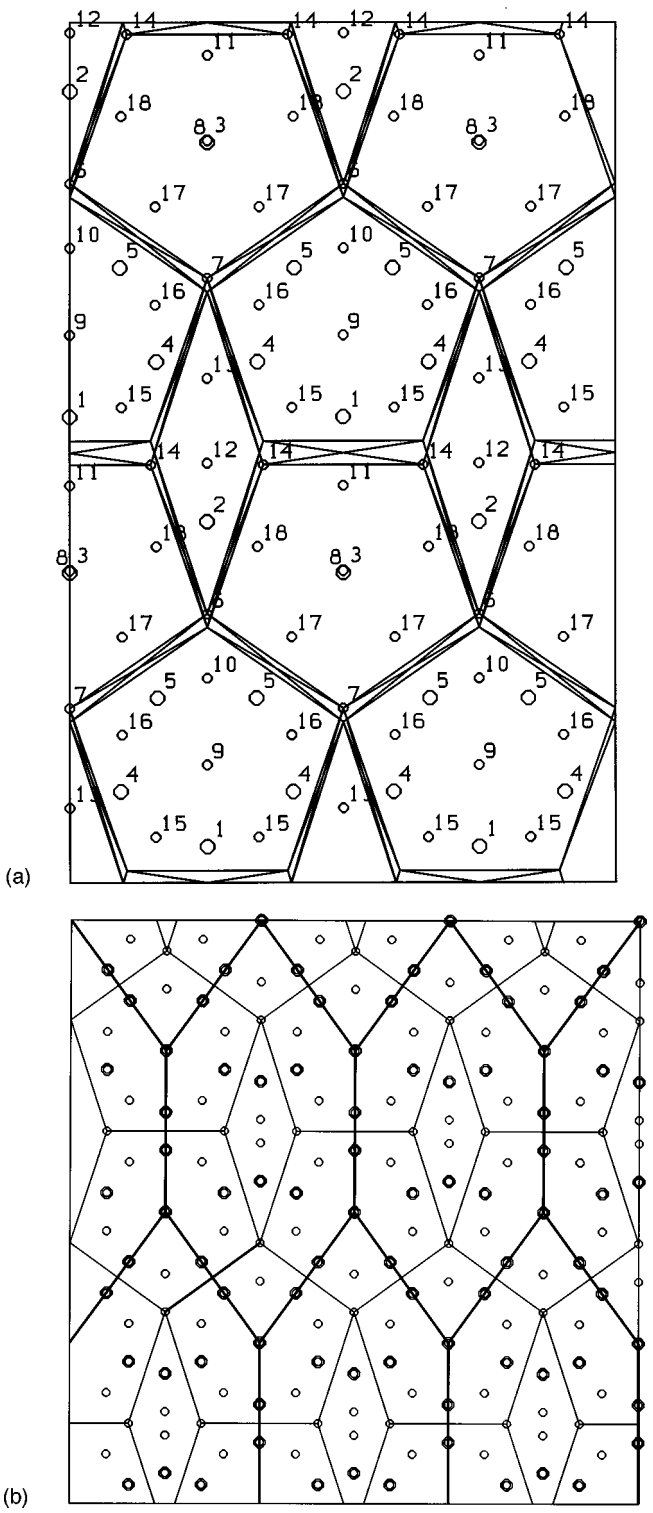

FIG. 7. Atomic structure of the *R* phase: (a) Projection of the positions of the atoms in half of the period on a plane perpendicular to the *c* axis (~ periodic axis in the quasiperiodic limit). Upper and lower halves of the cell are related through a twofold screw symmetry operation. Sites 1–5 (large circles) are occupied by Mn atoms, sites 6–18 (small circles) by Al atoms. The structure is drawn for two unit cells with the experimentally determined coordinates. (b) Projection of a full period of three unit cells. The thick lines show the *H* tiles, the thin lines the decomposition of the *H* tiles into small pentagonal columnar clusters and thin rhombi. Cf. text.

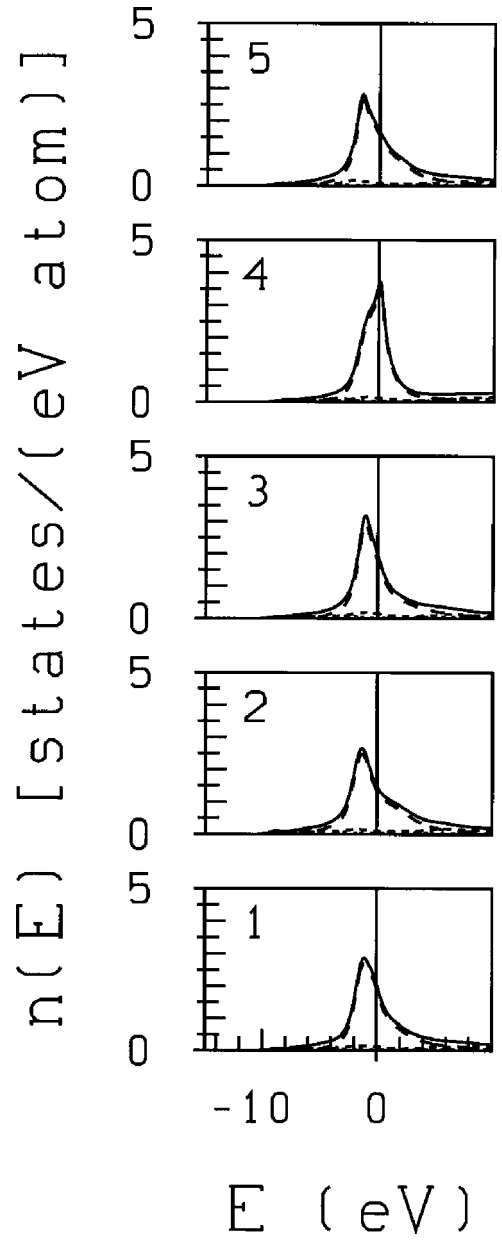

FIG. 8. Paramagnetic local densities of states on the Mn sites of the Al-Mn R phase, variant $V2$.

$a=7.75$ Å, $b=23.83$ Å, $c=12.43$ Å contains again 156 atoms. For the R phase exact atomic coordinates deviating slightly from the idealized geometry have been determined by single-crystal refinement,[55] and these coordinates have been used in our calculations. The atomic decoration is again based on the pentagonal columnar clusters, see Fig. 7. From the point of view of their positions within the pentagonal clusters, or the H tiles, respectively, we note the following equivalence between the Mn sites in the R and T phases: $1(R)\sim 2,4(T)$, $2(R)\sim 1(T)$, $3(R)\sim 7(T)$, $4(R)\sim 5,6(T)$, $5(R)\sim 3,4(T)$. Note that from the point of view of the tiling with pentagonal columnar clusters, the Mn sites fall into three categories: sites on the surface of the pentagonal columnar clusters (1, 4, 5 for R phase, 2–6 for the T phase), sites on the center axis of the clusters having only Al atoms in the outer shell $[3(R),7(T)]$, and sites in the region of thin rhombi $[2(R),1(T)]$. The three classes of sites differ in the

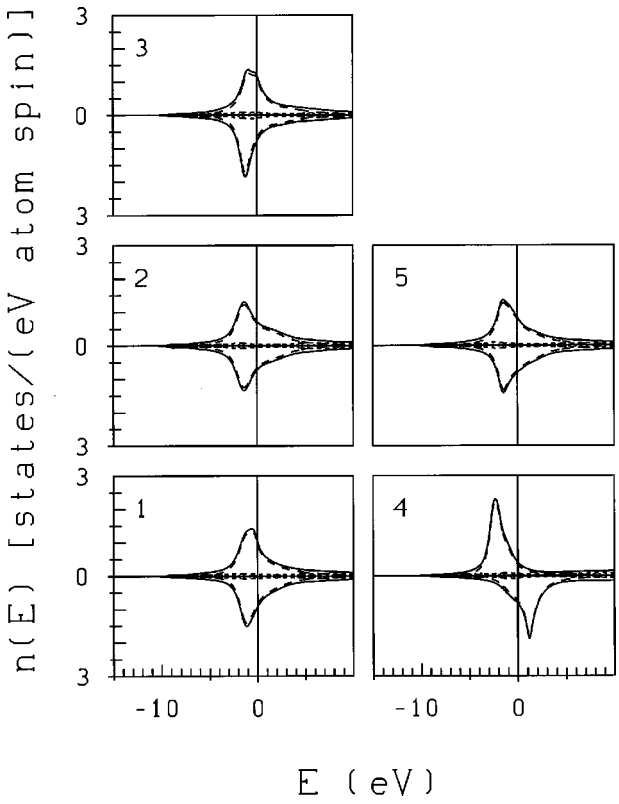

FIG. 9. Spin-polarized local densities of states on the Mn sites of the Al-Mn R phase, variant $V2$.

Mn-Mn coordinations: The average Mn-Mn coordination number is always 1.5, but Mn atoms on the periphery of the pentagonal clusters have at least two other Mn nearest neighbors within the same cluster. Site 4 (R phase) and sites 5 and 6 (T phase) have a third Mn neighbor in the next cluster. Sites on the center axis of the Al clusters and Mn sites within the rhombi have no direct Mn neighbors. The number of Al neighbors around Mn is 10, except for the center site which has 12 Al neighbors. However, around the sites with 3 Mn-Mn neighbors, the average Mn-Al distance is distinctly larger than on the other sites. This difference is larger in the R than in the T phase, the average Mn-Al distance varies between 2.51 Å [around Mn(1)] and 2.67 Å [around Mn(4)].

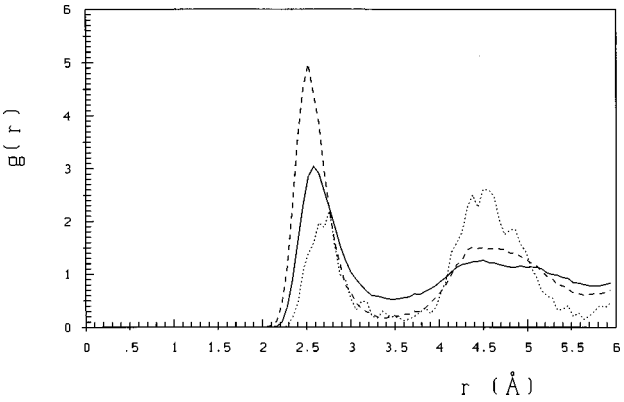

FIG. 10. Partial pair-correlation functions of liquid $Al_{0.86}Mn_{0.14}$ at $T=1300$ K as calculated using molecular dynamics. Full lines indicate Al-Al, dashed lines indicate Al-Mn, dotted lines indicate Mn-Mn correlations. Cf. text.

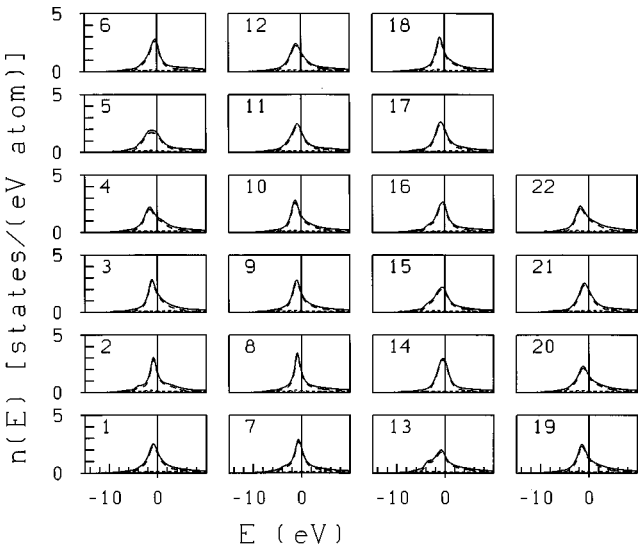

FIG. 11. Paramagnetic local densities of states at the Mn sites in a 154-atom ensemble representing liquid $Al_{0.86}Mn_{0.14}$.

Hence we note that the tendency to form a magnetic moment on sites 5 and 6 of the *T* phase is evidently related to a high Mn-Mn coordination. Note that while the distribution of Al and Mn sites on the five- and tenfold rings is fixed by symmetry, Al and Mn occupations can be interchanged in the rhombi. In the following we discuss the electronic and magnetic structure for two slightly different decorations of the *R* phase. Variant *R*-*V*1 is shown in Fig. 7(a), and in the variant *R*-*V*2 the occupation of sites 2 and 13 by Mn and Al is interchanged. The interchange of 2 and 13 increases the Mn-Mn coordination number on site 4 to five, while the Mn site within the rhombi has now two Mn neighbors in the adjacent pentagonal clusters.

The spin-polarized DOS of the *R*-*V*1 phase of Al-Mn is very similar to that of *T* phase (see Fig. 6), considering the equivalence listed above: on site 4 ($\sim$ sites 5, 6 in the *T* phase) the local Stoner criterion is marginally satisfied and spin-polarized calculation converges to a small moment on this site ($\mu_4 = 0.30\mu_B$), the moments on the other sites scatter between -0.03 and $+0.05\mu_B$.

TABLE II. Magnetic moments (in μ_B) on the Mn sites in a representative configuration of the 154-atom ensemble representing liquid $Al_{0.86}Mn_{0.14}$. The numbering of the sites is the same as in the graphs showing the electronic DOS.

Site No.	Local moment	Site No.	Local moment
1	0.004	12	0.002
2	−0.001	13	0.017
3	0.034	14	2.671
4	0.009	15	0.018
5	−0.033	16	1.534
6	1.795	17	−0.101
7	−0.717	18	−0.004
8	0.054	19	0.007
9	0.041	20	−0.004
10	−0.020	21	0.021
11	−0.023	22	−0.008

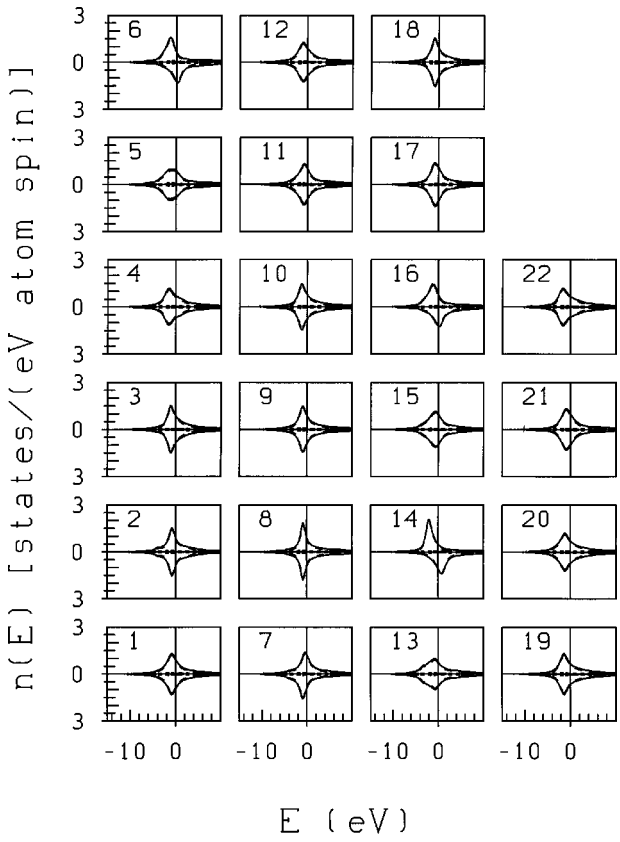

FIG. 12. Spin-polarized local densities of states at the Mn sites of a representative configuration of liquid $Al_{0.86}Mn_{0.14}$.

A large moment on site 4 is obtained if the occupation of sites 2 and 13 with Mn and Al is interchanged (model *R*-*V*2). This results in a local paramagnetic DOS at site 4 that is sharply peaked at the Fermi level (Fig. 8). The spin-polarized calculation converges to a large local moment $\mu_4 = 3.3\mu_B$ (see Fig. 9 for the spin-polarized DOS), a substantial antiferromagnetic moment is also formed on site 3 ($\mu_3 = -0.51\mu_B$), although the local Stoner criterion is just not satisfied. The other Mn moments are $\mu_1 = 0.06\mu_B$, $\mu_2 = -0.06\mu_B$. This confirms the important role of direct Mn-Mn neighbors for formation of a local moment. In addition a

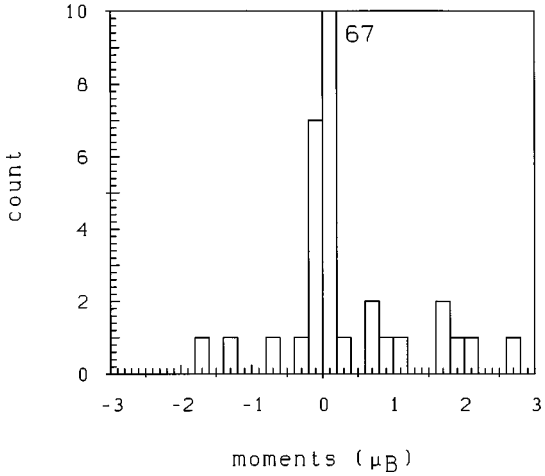

FIG. 13. Distribution of the local magnetic moments of the Mn atoms in liquid $Al_{0.86}Mn_{0.14}$.

looser packing of the Al atoms around the Mn atoms reduces the Al-p −Mn-d hybridization and leads to an impuritylike DOS on the central Mn site, similarly to what had been found in the fcc-solid solution.

On the other hand, the site symmetry plays a minor role in the formation of a magnetic moment: all Mn sites except the one at the center of the pentagonal cluster (which remains nonmagnetic) have very low symmetry.

V. LIQUID AL-MN ALLOYS

Model structures for liquid $Al_{0.86}Mn_{0.14}$ have been prepared by molecular-dynamics simulations, using the pair potentials proposed by Phillips *et al.*[59] These potentials have already been used with good success to study the dispersion relations for collective vibrational excitations in decagonal Al-Mn.[60] The simulations have been started at 2000 K. After an initial equilibration at high temperature, the alloy was cooled to 1300 K and re-equilibrated before data sampling. The simulations were performed for large ensembles with 756 atoms and small ensembles of 154 atoms. Spin-polarized electronic-structure calculations were performed for four selected configurations of the smaller ensembles, chosen such that the partial pair-correlation functions agree with the configuration average over the large ensemble.

The partial pair-correlation functions are shown in Fig. 10. The most striking features are the low amplitude of the first peak in the Mn-Mn correlation function and the dominant Al-Mn peak, as well as the deep minimum of these two correlation functions between the first and second peak. The Al-Al correlations on the other hand are similar to that of a dense random packing liquid. This is a clear signature of a preferred heterocoordination of the Mn atoms by Al (as in the crystalline and quasicrystalline alloys): on average each Mn atom has 11.45 nearest neighbors (calculated with a cutoff distance of 3.5 Å), only 0.98 of them are Mn (to be compared to a value of 1.6 Mn-Mn pairs for a random chemical distribution).

The electronic structure calculations have been performed self-consistently on all 22 Mn sites in the 154-atom cells, while the Al-potential parameters have been averaged over a representative sample of sites. The paramagnetic DOS on the Mn sites of configuration 1 is shown in Fig. 11. We find quite large variations in the shape and precise position of the Mn-d band. The local Stoner criterion for the formation of a magnetic moment is clearly satisfied on sites 6, 7, 14, and 16, on sites 2, 8, 11, 15, and 17 the DOS at E_F falls just below the limiting value. The spin-polarized calculations converge towards substantial moments just at these four sites (see Table II), on all other sites the moments remain essentially zero, although attempts have been made to induce a magnetic solution. The spin-polarized DOS's (Fig. 12) show the exchange-splitting and the non-rigid-band behavior on the magnetic sites.

Similar results are obtained for the other three configurations. The local Stoner criterion decides on the formation or absence of a local magnetic moments. Large moments fluctuating between -1.76 and $+2.67\mu_B$ on 14 Mn sites out of the total 88 sites, on the remaining sites $|\mu_i| \leqslant 0.2\mu_B$. The ensemble averages are $\langle \mu_i \rangle = 0.08\mu_B$, $\langle |\mu_i| \rangle = 0.30\mu_B$, the distribution of the local moments is shown in Fig. 13. The distribution of the magnetic moments with very large moments on some sites and small moments on the other sites is in a certain sense intermediate between the distributions found in the quasicrystalline approximants and in the fcc solid solution. The analysis of the local DOS's shows that on many sites the local Al-s,p −Mn-d hybridization in the liquid is still strong enough to broaden the local Mn-d −DOS and to shift it away from the Fermi level so that the formation of a local Mn moment is suppressed. If the spatial correlation between the orientation of the Mn moments is analyzed we find—admittedly with rather poor statistics—that nearest-neighbor moments tend to align antiferromagnetically, whereas second-nearest neighbors couple mostly ferromagnetically. In that sense l-AlMn behaves similarly to the fcc-solid solution, with a RKKY-like distance dependence of the effective Mn-Mn exchange interactions.

Our results are in qualitative agreement with the conclusions drawn from the susceptibility measurements and neutron scattering data on liquid $Al_{1-x-y}Pd_xMn_y$ ($y = 0.017 - 0.072$, $x \sim 0.20$) (Ref. 20) and on liquid $Al_{0.80}Mn_{0.20}$ (Ref. 61) that a fraction of the Mn atoms carry a large magnetic moment, while the remaining Mn sites are nonmagnetic. The estimated average moments, however are larger than obtained in our calculations. Part of the difference might be attributed to the interpretation of the neutron-scattering data: all intensity measured at low momentum was attributed to the paramagnetic scattering, on the ground that density fluctuations make an almost negligible contribution. This ignores the contribution from concentration fluctuations which can be quite large in a liquid with short-range chemical order. This would eventually lead to a lower average Mn moment.

We also have to note a striking disagreement with calculation of Bratkovsky *et al.*[36,37] The calculations were performed in a collinear and noncollinear mode. The collinear calculations converge towards a ferromagnetic solution where in l-$Al_{86}Mn_{14}$ *all* Mn sites carry a moment of $3.29\mu_B$. In the noncollinear calculations the size of the moments fluctuates between 2.6 and $3.3\mu_B$, but as the directions of the moments are oriented randomly in a spin-glass-like manner, an almost zero macroscopic polarization results. That *all* sites should carry large moments would imply that the local Stoner criterion should be satisfied on all sites—this would severely limit the possible variations in the local DOS. The absence of fluctuations in the local DOS would be a strange result that appears to be incompatible with the fluctuations in the local environment.

The reasons for the discrepancies between the calculations of Bratkovsky *et al.* and the present work are difficult to assess. Bratkovsky *et al.*[36,37] use a different set of interatomic potentials based on a semiempirical tight-binding approach. The average nearest-neighbor distances d_{ij} and coordination numbers Z_{ij}, however, compare quite well with the present results: $d_{\text{Mn-Mn}} = 2.77(2.83)$ Å, $d_{\text{Mn-Al}} = 2.59(2.59)$ Å, $d_{\text{Al-Al}} = 2.50(2.70)$ Å; $Z_{\text{Mn-Mn}} = 0.98(0.66)$, $Z_{\text{Mn-Al}} = 10.47(10.4)$ (values of Bratkovsky and Smirnov in parentheses). Hence structural differences cannot explain the different magnetic properties. Both sets of calculations have been performed using a real-space tight-binding LMTO method and the recursion method to calculate the local DOS's. Our calculation uses the Von Barth–Hedin form of

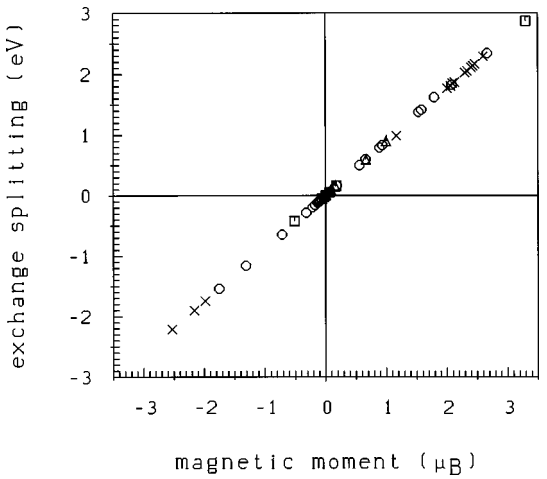

FIG. 14. Local magnetic moments μ_i versus local exchange splitting in all crystalline, quasicrystalline, and liquid Al-Mn alloys: crosses indicate the fcc-solid solution, rectangles indicate the *R* phase, triangles indicate the *T* phase, circles indicate the liquid alloy.

the LSDA exchange-correlation functional, no information on the LSDA functional used is given in the papers by Bratkovsky and Smirnov. Differences exist in the way the local self-consistent charge and spin densities and LMTO parameters are calculated. Concerning these aspects of the technique, Bratkovsky and Smirnov refer to their earlier work on amorphous Fe-B and Ni-B alloys[62] where the charge and spin densities were determined by taking the average over the central sites in a large cluster containing several hundred atoms. Hence the potential parameters are self-consistent only on average and this explains why the first of their calculations[36] on a large 666-atom cluster leads to the same moment of $\mu_{\mathrm{Mn}}=3.29\mu_B$ on all Mn sites in l-$Al_{86}Mn_{14}$, i.e., to a ferromagnetic solution. In the second paper Smirnov and Bratkovsky[37] claim to have achieved local self-consistency. However, no technical details and no results on the paramagnetic or spin-polarized local DOS's are given so that a more detailed analysis of a possible origin of the discrepancies in terms of different degrees of local Al-s,p −Mn-d hybridization is not possible. One possible reason why both sets of calculations converge to different magnetic states could also be in the initialization of the spin-polarized calculations. To break the symmetry of the paramagnetic state, the calculations must be initialized either with nonzero moments on some sites, or a small magnetic-field term must be added. From a number of calculations of disordered magnetic states[50,63,64] it is well known that different initializations can lead to very different metastable magnetic configurations which often differ only very little in energy. In our calculations we have adopted an initialization with small local moments (cf. Sec. II) because we are interested in the spontaneous formation of local moments. No information on this aspect of the calculations may be found in Smirnov and Bratkovsky.[37] It is conceivable, however, that an initiatilization with large magnetic moments converges to a metamagnetic high-spin solution.

VI. DISCUSSION AND SUMMARY

We have performed self-consistent local-spin-density calculations of the electronic and magnetic structure of crystalline, quasicrystalline (icosahedral and decagonal), and liquid Al-Mn alloys. We find that the formation of a magnetic moment is governed by a local Stoner criterion, i.e., a site is magnetic if $n_i(E_F)I>1$ and nonmagnetic if $n_i(E_F)I<1$. Here $n_i(E)$ is the local density of states and I is the Stoner intra-atomic exchange integral. (For an itinerant magnet it is determined primarily by Hund's rule exchange, see, e.g., Anisimov *et al.*[65]). The local magnetic moments μ_i and the local exchange splitting Δ_i are in this case related through $\Delta_i=I\mu_i$. If we define the local exchange splitting in terms of the difference in the center of gravity of the spin-up and spin-down bands (i.e., with the TB-LMTO in terms of the difference in the corresponding LMTO potential parameters) we find that a strictly linear relation between μ_i and Δ_i holds in all Al-Mn phases (Fig. 14). From the slope we derive an effective Stoner parameter of $I\sim 0.92$ eV/μ_B, i.e., within ± 0.01 eV/μ_B the same value as determined by Turek *et al.*[66] for a large number of Fe-, Co-, and Ni-based crystalline and amorphous phases and as derived by Himpsel[67] from photoemission and inverse photoemission experiments. This confirms that the driving mechanism is really an intra-atomic Hund's-rule exchange. The decisive factor is then the form of the local DOS on the Mn sites which is determined by the local Al-p −Mn-d hybridization and Mn-d −Mn-d interactions. Here we find a clear correlation with the structural properties:

(a) Al-p −Mn-d hybridization is strongest in the crystalline compound Al_6Mn where it enhances the structure-induced Hume-Rothery pseudogap at the Fermi level. In addition, the absence of direct Mn-Mn neighbors eliminates a possible direct exchange coupling. Hence the crystalline compound is clearly nonmagnetic.

(b) Hybridization effects are still comparatively strong in quasicrystalline alloys (both icosahedral and decagonal). However, quasiperiodicity allows for a wide variety of local environments and on certain sites the criterion for the formation of a local moment can be satisfied. We have demonstrated this explicitly for some low-order approximants to the icosahedral and decagonal phases. We have also shown that the decisive factor for local moment formation is an enhanced Mn-Mn coordination (which is found only in the decagonal, but not in the icosahedral phases) and a looser Mn-Al coordination. There is also clear evidence that magnetic moments will appear in quasicrystalline alloys only in a minority of the Mn sites, in agreement with experiment.

(c) Melting a quasicrystal or crystal does not completely destroy the short-range order. Consequently, in a liquid we have a broad distribution of local environments, corresponding to large fluctuations in the local DOS. Consequently, the Stoner criterion will be satisfied on some sites, but on other sites a strong local Al-p −Mn-d interaction will lead to a reduced DOS at the Fermi level and hence suppress the formation of a local moment. Again the predicted coexistence of nonmagnetic sites and sites with a large magnetic moment is in semiquantitative agreement with experiment.

(d) In a substitutionally disordered solid solution the confinement of the atoms to fixed interatomic spacing, irrespective of the local chemical environment, reduces the Al-p −Mn-d hybridization and leads to an impuritylike local DOS on the Mn-minority sites. The peak of Mn-DOS is pinned at the Fermi level (due to the half-filled Mn-band)

and hence all Mn sites carry large moments of fluctuating sign. Effectively, fcc Al-Mn is an Ising spin glass within the collinear LSDA calculation.

The very clear picture resulting from this analysis also settles some points discussed repeatedly in the literature: (i) Formation of local magnetic moments is definitely not related to icosahedral site symmetry. (ii) Formation of magnetic moments in the liquid phase is not induced by topological disorder—purely substitutional disorder is much more effective in promoting the formation of a local magnetic moment. The decisive factor is rather to break the strong Al-p−Mn-d hybridization which suppresses the magnetic instability in the crystalline structure and on almost all sites of the quasicrystalline lattices. Here we have shown that to arrange the atoms in a substitutionally disordered way on a perfect fcc lattice is much more effective in reducing the hybridization than an overall topological disorder allowing for a short-range order leading to stronger local hybridization.

A major challenge in the theory of the magnetic properties of quasicrystals, however, is still the explanation of the diamagnetism observed in many quasicrystals. We suspect (but cannot prove as yet) that the diamagnetism is closely related to the unusual transport properties of quasicrystals, and hence to the character of the electronic eigenstates close to the Fermi level. Further investigations will be needed to explore this correlation.

ACKNOWLEDGMENTS

J.H. acknowledges clarifying discussions with Dr. R. Zeller. This work has been supported by the Hochschuljubiläumsfonds der Österreichischen Nationalbank (Project No. ÖNB 5608) and by the Bundesministerium für Wissenschaft, Forschung und Kunst (Project: ''Magnetism on Nanometer Scale'').

*Permanent address: Institute of Physics, Slovak Academy of Sciences, SK 84228 Bratislava, Slovakia.

[1] For recent reviews see, e.g., S. J. Poon, Adv. Phys. **41**, 303 (1992); Ch. Janot, *Quasicrystals–A Primer*, 2nd ed. (Oxford University Press, Oxford, 1995).

[2] J. J. Hauser, H. S. Chen, and J. V. Waszczak, Phys. Rev. B **33**, 3577 (1986).

[3] R. A. Dunlap, M. E. McHenry, V. Srinivas, D. Bahadur, and R. C. O'Handley, Phys. Rev. B **39**, 4808 (1989).

[4] A. P. Tsai, A. Inoue, T. Masumoto, and N. Kataoka, J. Appl. Phys. **27**, L2252 (1988).

[5] J. G. Zhao, L. Y. Yang, Q. Fu, and H. Q. Guo, Proc. Jpn. Inst. Metals **29**, 497 (1988).

[6] Z. M. Stadnik and G. Stroink, Phys. Rev. B **43**, 894 (1991).

[7] Z. M. Stadnik, G. Stroink, H. Ma, and G. Williams, Phys. Rev. B **39**, 9797 (1989).

[8] M. Eibschütz, M. E. Lines, H. S. Chen, J. W. Waszczak, G. Papaefthymion, and R. B. Frankel, Phys. Rev. Lett. **59**, 2443 (1987).

[9] W. W. Warren, H. S. Chen, and G. P. Espinosa, Phys. Rev. B **34**, 4902 (1986).

[10] J. J. Hauser, H. S. Chen, G. P. Espinosa, and J. W. Waszczak, Phys. Rev. B **34**, 4674 (1986).

[11] Z. B. Stadnik, Hyperfine Interact. **90**, 215 (1990).

[12] C. Berger, J. C. Lasjaunias, J. L. Tholence, D. Pavuna, and P. Germi, Phys. Rev. B **37**, 6525 (1988).

[13] C. Berger and J. J. Prejean, Phys. Rev. Lett. **64**, 1769 (1990).

[14] M. A. Chernikov, A. Bernasconi, C. Beeli, A. Schilling, and H. R. Ott, Phys. Rev. B **48**, 3058 (1993).

[15] M. Godinho, C. Berger, J. C. Lasjaunias, K. Hasselbach, and O. Berthoux, J. Non-Cryst. Solids **117-118**, 808 (1990).

[16] T. Klein, C. Berger, D. Mayou, and F. Cyrot-Lackmann, Phys. Rev. Lett. **66**, 2907 (1991).

[17] S. Matsuo, H. Nakano, T. Ishimasa, and Y. Fukano, J. Phys.: Condens. Matter **1**, 6893 (1989).

[18] K. Saito, S. Matsuo, and T. Ishimasa, J. Phys. Soc. Jpn. **62**, 604 (1993).

[19] P. Lanco, T. Klein, C. Berger, F. Cyrot-Lackmann, G. Fourcaudot, and A. Sulpice, Europhys. Lett. **18**, 227 (1992).

[20] F. Hippert, M. Audier, H. Klein, R. Bellissent, and D. Boursier, Phys. Rev. Lett. **76**, 54 (1996).

[21] R. Lück and S. Kek, J. Non-Cryst. Solids **193-194**, 329 (1993).

[22] M. E. McHenry, D. D. Vvedensky, M. E. Eberhart, and R. C. O'Handley, Phys. Rev. B **46**, 495 (1992).

[23] S. S. Jaswal and X. G. He, Phys. Rev. B **46**, 495 (1992).

[24] F. Liu, S. N. Khanna, L. Magaud, P. Jena, V. De Coulon, F. Reuse, S. S. Jaswal, X. G. He, and F. Cyrot-Lackmann, Phys. Rev. B **48**, 1295 (1993).

[25] T. Fujiwara and T. Yokokawa, Phys. Rev. Lett. **66**, 333 (1991).

[26] J. Hafner and M. Krajčí , Phys. Rev. Lett. **68**, 2321 (1992).

[27] M. Krajčí, M. Windisch, J. Hafner, G. Kresse, and M. Mihalkovič, Phys. Rev. B **51**, 17 355 (1995).

[28] V. L. Moruzzi and P. M. Marcus, Phys. Rev. B **45**, 2934 (1992); **47**, 7878 (1993).

[29] E. Belin-Ferré, Z. Dankházi, A. Sadoc, and J. M. Dubois, J. Phys.: Condens. Matter **6**, 8771 (1994).

[30] G. W. Zhang, Z. M. Stadnik, A. P. Tsai, and A. Inoue, Phys. Lett. A **186**, 345 (1994).

[31] M. Krajčí, J. Hafner, and M. Mihalkovič, Europhys. Lett. **34**, 207 (1996); Phys. Rev. B **55**, 843 (1997).

[32] M. Krajčí, J. Hafner, and M. Mihalkovič, Phys. Rev. B **56**, 3072 (1997).

[33] Z. M. Stadnik, G. W. Zhang, A. P. Tsai, and A. Inoue, Phys. Lett. A **198**, 237 (1995); Phys. Rev. B **51**, 11 358 (1995).

[34] E. Belin-Ferré, Z. Dankházi, V. Fournée, A. Sadoc, C. Berger, H. Müller, and H. Kirchmayr, J. Phys.: Condens. Matter **8**, 6213 (1996).

[35] Z. M. Stadnik, D. Purdie, M. Garnier, Y. Baer, A. P. Tsai, A. Inoue, K. Edagawa, S. Takeuchi, and K. H. J. Buschow, Phys. Rev. B **55**, 10 938 (1997).

[36] A. M. Bratkovsky, A. V. Smirnov, D. Nguyen Mahn, and A. Pasturel, Phys. Rev. B **52**, 3056 (1995).

[37] A. V. Smirnov and A. M. Bratkovsky, Phys. Rev. B **53**, 8515 (1996).

[38] U. von Barth and L. Hedin, J. Phys. C **4**, 2064 (1972).

[39] O. K. Andersen and O. Jepsen, Phys. Rev. Lett. **53**, 2571 (1984).

[40] O. K. Andersen, O. Jepsen, and M. Šob, in *Electronic Band Structure and its Applications*, edited by M. Youssouff (Springer, Berlin, 1987).

[41] S. K. Bose, S. S. Jaswal, O. K. Andersen, and J. Hafner, Phys. Rev. B **37**, 9955 (1988).
[42] V. Heine, D. Bullett, R. Haydock, and M. J. Kelly, in *Solid State Physics: Advances in Research and Applications*, edited by H. Ehrenreich, D. Turnbull, and F. Seitz (Academic, New York, 1980), Vol. 35.
[43] M. U. Lucchini and C. M. M. Nex, J. Phys. C **20**, 3125 (1987).
[44] A. D. I. Nicol, Acta Crystallogr. **9**, 285 (1953).
[45] G. Trambly de Laissardière, D. Nguyen Manh, L. Magaud, J. P. Julien, F. Cyrot-Lackmann, and D. Mayou, Phys. Rev. B **52**, 7920 (1995); G. Trambly de Laissardière, D. Mayou, and D. Nguyen Manh, Europhys. Lett. **21**, 25 (1993).
[46] J. Deutz, P. H. Dederich, and R. Zeller, J. Phys. F **11**, 1787 (1981).
[47] R. M. Nieminen and M. Puska, J. Phys. F **10**, L123 (1980).
[48] T. Hoshino, R. Zeller, and P. Dederichs, Phys. Rev. B **53**, 8971 (1996).
[49] R. Zeller and P. Dederichs (private communication).
[50] Ch. Becker, J. Hafner, and R. Lorenz, J. Magn. Magn. Mater. **157-158**, 619 (1996).
[51] See, e.g., K. H. Fischer and J. A. Hertz, *Spin Glasses* (Cambridge University Press, Cambridge, 1991).
[52] A. Waseda, H. Morioka, K. Kimura, and H. Ino, Philos. Mag. Lett. **65**, 25 (1992).
[53] E. Cockayne, R. Phillips, X. B. Khan, S. C. Moss, J. L. Robertson, T. Ishimasa, and M. Mori, J. Non-Cryst. Solids **153-154**, 140 (1993).
[54] M. A. Taylor, Acta Crystallogr. **14**, 84 (1961).
[55] K. Robinson, Acta Crystallogr. **7**, 494 (1954).
[56] C. Beeli and S. Horiuchi, Philos. Mag. B **70**, 215 (1994).
[57] K. Hiraga and W. Sun, Philos. Mag. Lett. **67**, 117 (1993).
[58] K. Hiraga, M. Kaneko, Y. Matsuo, and S. Hashimoto, Philos. Mag. B **67**, 193 (1993).
[59] R. Phillips, J. Zou, A. C. Carlsson, and M. Widom, Phys. Rev. B **49**, 9322 (1994).
[60] J. Hafner, M. Krajčí, and M. Mihalkovič, Phys. Rev. Lett. **76**, 2738 (1996).
[61] M. Maret, P. Chieux, J. M. Dubois, and A. Pasturel, J. Phys.: Condens. Matter **3**, 2801 (1991); M. Maret, A. Pasturel, C. Senillou, J. M. Dubois, and P. Chieux, J. Phys. (Paris) **50**, 295 (1989).
[62] A. M. Bratkovsky and A. V. Smirnov, Phys. Rev. B **48**, 9606 (1993); J. Phys.: Condens. Matter **5**, 3203 (1993).
[63] D. Spišák, J. Hafner, and R. Lorenz, J. Magn. Magn. Mater. **166**, 303 (1997).
[64] M. Liebs and M. Fähnle, Phys. Rev. B **53**, 14 012 (1996).
[65] V. I. Anisimov, J. Zaanen, and O. K. Andersen, Phys. Rev. B **44**, 943 (1991).
[66] I. Turek, Ch. Becker, and J. Hafner, J. Phys.: Condens. Matter **4**, 7257 (1992).
[67] F. J. Himpsel, Phys. Rev. Lett. **67**, 2363 (1991).